Journal of Photochemistry, 11 (1979) 27 - 37

PHOTOCHEMICAL MECHANISMS FOR PHOTOGALVANIC CELLS PART 6: THE IRON–THIONINE SYSTEM

W. JOHN ALBERY† and W. RICHARD BOWEN
Physical Chemistry Laboratory, South Parks Road, Oxford (Gt. Britain)
MARY D. ARCHER‡ and M. ISABEL FERREIRA*
The Royal Institution, 21 Albermarle Street, London, W1 (Gt. Britain)
(Received October 27, 1978)

Summary

Results are presented for the composition of the photostationary state in the iron–thionine photo-redox system as a function of the concentration of Fe(II) and Fe(III) and of the irradiance of the light. From these results the mechanism of the photo-redox system can be deduced. It is shown that depending on the conditions two of the possible six mechanisms are found. The implications for the efficient conversion of solar energy into electrical energy are discussed.

1. Introduction

In the previous paper [1] we showed that there were six different possible mechanisms for a one electron–two electron photo-redox system. In this paper we describe experiments on the photostationary state of the iron–thionine system and show how we can deduce the photochemical mechanism from such studies. Depending on the conditions, the system reacts by two of the six possible mechanisms; the implications of these findings for solar energy conversion are also discussed.

The reaction scheme for the iron–thionine photo-redox system in the notation of part 5 is

$$A + Z \underset{k_{-1}}{\overset{g}{\rightleftharpoons}} B + Y$$

†Present address: Department of Chemistry, Imperial College, London SW7 2AY, Gt. Britain.
‡Present address: Department of Physical Chemistry, Lensfield Road, Cambridge, Gt. Britain.
*Present address: University of Minho, Braga, Portugal.

$$B + Z \underset{k_{-2}}{\overset{k_2}{\rightleftharpoons}} C + Y$$

$$B + B \underset{k_{-3}}{\overset{k_3}{\rightleftharpoons}} A + C$$

where A is

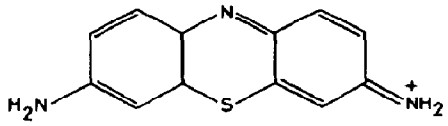

B is

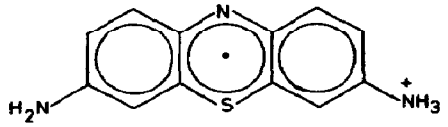

C is

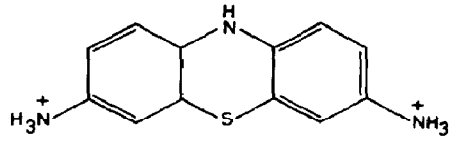

Z is Fe(II) and Y is Fe(III). The thermal reactions have the rate constants as shown and the photochemically driven process (A + Z → B + Y) has a flux g.

The photostationary state has been investigated in two different media: the first consists of 0.05 M H_2SO_4 and the second of 0.1 M K_2SO_4 adjusted to a pH of 2.5 by addition of H_2SO_4 (about 10^{-3} M). The concentration of Fe(II) was varied from 0.5 mM to 50 mM and that of Fe(III) from 10^{-2} mM to 5 mM. The irradiance was varied by a factor of 10. Under the different conditions the amount of conversion of A to C in the photostationary state was measured.

2. Experimental

The experiments have been carried out on two different sets of apparatus, one at the Physical Chemistry Laboratory in Oxford and one at the Royal Institution in London. In the Oxford experiments a uniform parallel beam of light from a 250 W tungsten–halogen projector lamp was filtered and shone on to a 1 cm optical cell. The irradiance was varied by using neutral density filters. The cell was jacketted and thermostatted to 25.0 °C. The light

passed through the cell, a Spex Micromate monochromator set to λ = 597 nm, and thence to an RS 305-462 photodiode. The concentration of thionine in the cell was determined from the photodiode reading which was calibrated using known concentrations of thionine. The same type of apparatus was used at the Royal Institution except that the optical length of the cell was 0.5 cm, the light source was a 500 W tungsten–halogen lamp, an Applied Photophysics monochromator and Hakuto photomultiplier were used and finally the experiments were carried out at room temperature (22 ± 2 °C).

Irradiance was measured in Oxford using a Hewlett Packard 8330A radiant fluxmeter. The calibration of the fluxmeter was checked at two different wavelengths using ferrioxalate actinometry [2]. Irradiance was measured in London by means of a Hilger Schwartz FT 15 thermopile.

All water was doubly distilled. All chemicals except thionine were of AnalaR grade. In Oxford thionine was supplied by Fluka and was used after insoluble impurities had been filtered. In London thionine (Eastman Kodak Co.) was purified chromatographically on a column of alkaline alumina using 95% ethanol as eluent [3]. The thionine fraction was evaporated to dryness and was shown to be free of its initial impurities by thin layer chromatography.

3. Results and discussion

3.1. The photochemical flux g

We start by considering the photochemically driven flux g of the reaction of thionine (A) and Fe(II)(Z). The solutions were irradiated with polychromatic light from a wavelength range λ_1 - λ_2 where the thionine absorption band lies between these wavelengths. It can be shown that

$$g = \theta \frac{[A]}{[A]_D} \varphi_B g_0 \tag{1}$$

$$\text{where } g_0 = [A]_D \int_{\lambda_1}^{\lambda_2} \epsilon_\lambda E_\lambda \frac{\lambda}{Lhc} \, d\lambda \tag{2}$$

θ is the fraction of light transmitted by the neutral density filter, $[A]_D$ is the concentration of A in the dark, φ_B is the quantum efficiency for the production of B, g_0 is the value of g for an unbleached solution and no neutral density filter and $\varphi_B = 1$, ϵ_λ is the natural molar extinction coefficient for thionine, and E_λ is the spectral irradiance in units of W cm^{-2} nm^{-1}.

The spectral irradiance is found from the readings F (W cm^{-2}) of the fluxmeter on the thermopile:

$$E_\lambda = \frac{F(\lambda)F_\Sigma}{\int_{\lambda_1}^{\lambda_2} F(\lambda) d\lambda}$$

where $F(\lambda)$ is the reading after the output of the lamp has passed through the monochromator and F_Σ is the reading for all the light between λ_1 and λ_2.

The results for the concentrations of thionine and for g_0 are given in Table 1.

TABLE 1

Results for the concentration of thionine and g_0

Medium	Oxford 0.05 M H_2SO_4	London 0.10 M K_2SO_4 at pH 2.5
$[A]_D$ (μM)	7.8	30
g_0 (mM s^{-1})	0.41	0.083

3.2. Identification of the mechanism

We define a bleaching ratio f which describes how much leucothionine is formed in the photostationary state:

$$f = [C]/[A]_D \tag{3}$$

The first step in analysing the results is to find which of the six mechanisms [1] apply for the system. This is done by testing the way in which [C] varies with [Y] and the irradiances I (in units of mol cm^{-2} s^{-1}) as given in Table 2 of part 5 [1]. We do not at first use the dependence on [Z] because the quantum efficiency φ_B also depends on [Z]. We therefore choose a value of [Z] which is kept constant for a set of experiments. Since [Z] $\gg$ [A], the concentration of Fe(II) (Z) is not significantly perturbed in the photostationary state. We then measure values of f for different values of [Fe(III)] (Y) and of our different neutral density filters of transmittance θ. Because of the bleaching of the solution the concentration of thionine (A) will not be constant for all experimental points. For each neutral density filter we then plot log $\{f/(1-f)\}$ against log [Fe(III)]. We choose a value of f and for each neutral density filter we find by interpolation the value of [Fe(III)] which corresponds to the chosen value of f. Typical results are shown in Fig. 1. Thus by this procedure we find a set of values of θ and of [Fe(III)] which give the same value of f. Neglecting the very small concentration of semithionine present [1, 4] the sum of the thionine and leucothionine concentrations is constant throughout; then all points with the same value of f will have the same values of [A] and [C].

We can now use Fig. 1 of part 5 which depicts the complete set of mechanisms. In that figure the normalized photochemical flux γ is plotted as the vertical axis. From eqns. (1) and (3)

$$\log \gamma = \text{constant} + \log \{\theta(1-f)\} \tag{4}$$

We explore how log γ or log $\{\theta(1-f)\}$ varies with log {Fe(III)} under conditions where [Fe(II)], [A] and [C] are held constant. The results obtained by interpolation at constant values of f are also shown in Fig. 1. This is equiv-

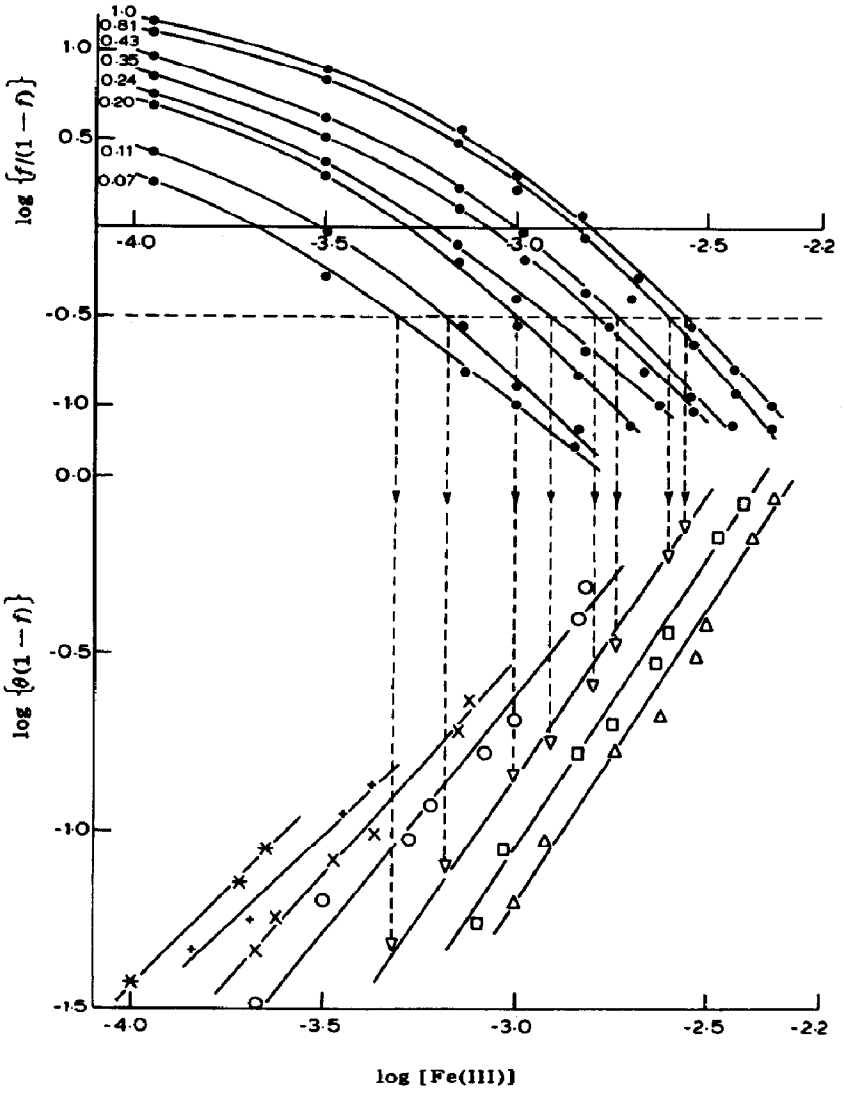

Fig. 1. The upper half of the figure shows typical experimental data obtained with [Fe(II)] = 0.5 mM and [thionine] = 7.8 μM. Each line corresponds to a particular neutral density filter and is labelled with the relative light intensity θ. The points show the observed bleaching of the solution as a function of [Fe(III)]. The lower half of the diagram shows the first part of the analysis where, at a chosen constant value of f, values of $\theta(1-f)$ are plotted as a function of [Fe(III)]. The procedure is indicated by the broken lines for $f = 0.24$. The different symbols correspond to the following values of f for each line: *, 0.91; +, 0.86; ×, 0.76; ○, 0.50; △, 0.24; □, 0.14; △, 0.091.

alent to constructing log–log plots on the slices shown in Fig. 1 of part 5. From the results in Table 2 of part 5 we can deduce for each mechanism the gradients of the plots and how the separation of the lines depends on f. The results are given in Table 2. Apart from the A2 B2 C1 and A2 B2 C2 mechanisms each mechanism has unique characteristics.

TABLE 2

Gradients and separation of log $\{\theta(1-f)\}$ *vs.* log [Fe(III)] plots

Mechanism	Gradient	Separation
A1 B1 C1	2.0	$\Delta \log f$
A1 B2 C1	1.5	$\frac{1}{2}\Delta \log f$
A1 B2 C2	1.0	$\Delta \log \{f(1-f)\}^{1/2}$
A2 B1 C1	2.0	$2\Delta \log f$
A2 B2 C1 A2 B2 C2	1.0	$\Delta \log f$

In Table 3 we report the gradients of the plots in Fig. 1 and also those at other [Fe(II)]. In 0.05 M H_2SO_4 for each [Fe(II)] the gradients are close to unity on the left-hand side of Fig. 1 at low [Fe(III)] and they rise to about 1.5 on the right-hand side at high [Fe(III)]. Inspection of Fig. 1 in part 5 [1] together with the values in Table 2 shows that this pattern is found if with increasing [Fe(III)] the system is crossing either the plane OPUT from A2 B2 C1 to A1 B2 C1 or the plane OPW from A1 B2 C2 to A1 B2 C1.

To decide between A2 B2 C1 and A1 B2 C2 we examine the separation of the lines in Fig. 1 on the left-hand side and we find that it is given by $\Delta \log f$. This shows that at the lower [Fe(III)] the mechanism is A2 B2 C1 and not A1 B2 C2. The data in 0.1 M K_2SO_4 differs from that in 0.05 M H_2SO_4 in that the gradient changes from 1.0 to 1.5 at much lower values of f. Hence the A2 B2 C1 mechanism is more dominant for these data.

We can now test the mechanistic identification by removing the separation between the various sets of data at different values of f using the appropriate function in Table 2. Thereby we collapse all the data onto the $f = 0.50$ line by plotting the functions of θ and f given in eqns. (5) and (6):

TABLE 3

Values of the gradients in Fig. 1

[Fe(II)] (mM)							
0.05 M H_2SO_4	f						
	0.91	0.86	0.76	0.50	0.24	0.14	0.091
50	1.2	1.2	1.3	1.3	1.5	–	–
5	1.1	1.1	1.2	1.3	1.5	–	–
0.5	1.1	1.0	1.2	1.3	1.6	1.6	1.6
0.10 M K_2SO_4	f						
	0.71	0.62	0.5	0.39	0.29		
10	0.95	0.80	0.90	0.94	1.1		

$$\text{A2 B2 C1} \qquad \theta_2 = \log\{\theta(1-f)\} - \log(2f) = \log\left\{\frac{\theta(1-f)}{2f}\right\} \tag{5}$$

$$\text{A1 B2 C1} \qquad \theta_1 = \log\{\theta(1-f)\} - \tfrac{1}{2}\log(2f) = \log\left\{\frac{\theta(1-f)}{(2f)^{1/2}}\right\} \tag{6}$$

Typical plots are shown in Fig. 2 for 0.05 M H_2SO_4. For each [Fe(II)] we find that on the left-hand side the data lie on a common line of gradient 1.0 and on the right-hand side on a common line of gradient 1.5. This agrees with the values in Table 2 and therefore completes the identification of the mechanisms. Our conclusions agree with those of Hatchard and Parker [5], of Ferreira and Harriman [4] and of Wildes *et al.* [6]. Their approach involved extensive flash photolysis experiments to determine individual rate constants. In this work we show how analysis of the simpler photostationary state experiments can elucidate the mechanistic information.

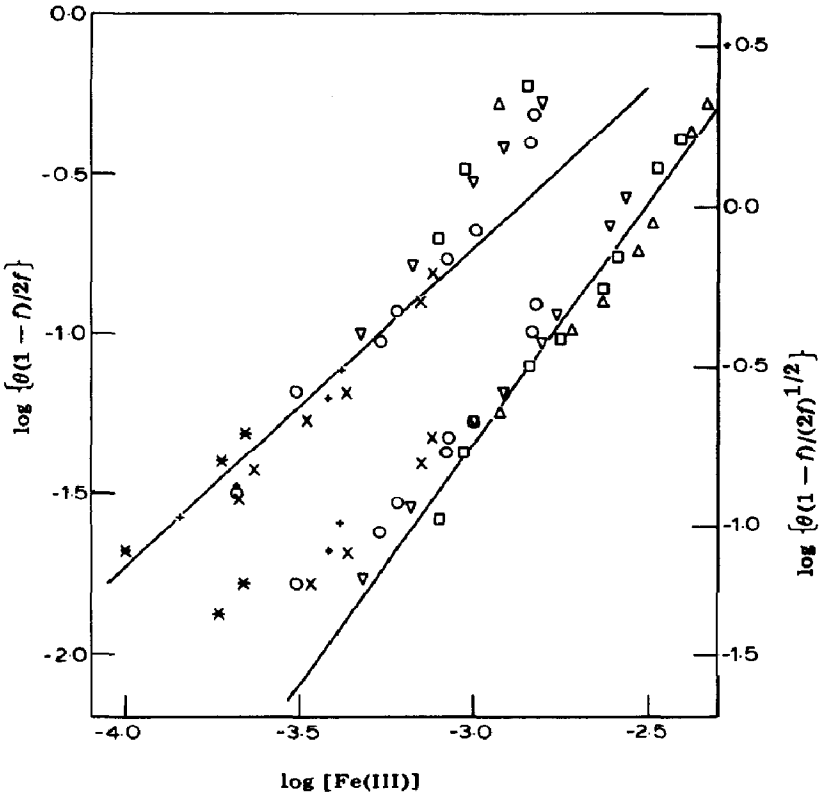

Fig. 2. Typical plots of eqns. (5) and (6) for the data plotted in Fig. 1. The symbols are the same as in Fig. 1.

3.3. *The dependence of the quantum efficiency on [Fe(II)]*

In Table 4 we report values of θ_2 and θ_1 in 0.05 M H_2SO_4 at [Fe(III)] = 1 mM but at different [Fe(II)]. From Table 2 of part 5 [1] we find that

apart from φ_B the bleaching should be independent of [Fe(II)] and from eqns. (1), (4) - (6)

$$\left(\frac{\partial\theta_n}{\partial[\mathrm{Fe(II)}]}\right)_{[\mathrm{Fe(III)}]} = -\left(\frac{\partial \log\varphi_B}{\partial[\mathrm{Fe(II)}]}\right)_{[\mathrm{Fe(III)}]} \tag{7}$$

Thus the variation of θ_n in Table 4 is caused by the effect of Fe(II) on φ_B and not its involvement in the subsequent steps. The only significant routes for the removal of triplet thionine A* in our experimental conditions are radiationless triplet decay and reaction with Fe(II) (Z):

$$A^* \xrightarrow[k_*]{} A$$

$$A^* + Z \xrightarrow[k_q]{} B + Y$$

then

$$\varphi_B = \frac{\varphi_{A^*}}{1 + K_q/[\mathrm{Fe(II)}]} \tag{8}$$

where $K_q = k_*/k_q$ and φ_{A^*} is the quantum efficiency for the production of A*. Given two values of θ_n at two different concentrations of Fe(II), from eqn. (7) we can write

$$\log(\varphi_{B,I}/\varphi_{B,II}) = \theta_{n,II} - \theta_{n,I} \tag{9}$$

and from eqn. (8)

$$K_q = \left(\frac{\varphi_{B,I}}{\varphi_{B,II}} - 1\right)\left(\frac{1}{[\mathrm{Fe(II)}]_{II}} - \frac{\varphi_{B,I}/\varphi_{B,II}}{[\mathrm{Fe(II)}]_I}\right)^{-1} \tag{10}$$

Results for K_q are given in Table 5. Reasonable agreement is found between the different sets of data. The result of 3.5 depends on a set of data where the A2 B2 C1 mechanism is not very dominant and the value is therefore likely to be less well determined. Otherwise the agreement in K_q further supports the mechanistic identification. The value of K_q in Table 5 of 5 mM is in reasonable agreement with Hatchard and Parker's [5] value of K_q = 2 mM and Ferreira and Harriman's value [4] in 0.1 M K_2SO_4 of 1 mM. The flash photolysis experiments were carried out at room temperature whereas the results in Table 5 were obtained at 25 °C.

TABLE 4

Values of θ_1 and θ_2 at [Fe(III)] = 1 mM

[Fe(II)] (mM)	A2 B2 C1	A2 B2 C2
50	−1.59	−1.73
5.0	−1.46	−1.48
0.5	−0.71	−0.73

TABLE 5

Values of K_q (mM) from eqns. (9) and (10) and data in Table 4

$[Fe(II)]_I$ (mM)	$[Fe(II)]_{II}$ (mM)	A2 B2 C1	A1 B2 C2
5	0.5	5.2	5.2
50	0.5	(3.5)	5.0

3.4. *Evaluation of rate constants and boundary conditions*

To evaluate the rate constants we can now plot all the data in a particular medium on a common graph. It can be shown for the two mechanisms A1 B2 C1 and A2 B2 C1 that

$$k_{-2} + k_{-1}\left(\frac{k_{-2}}{k_3}\frac{[Fe(III)]}{[C]}\right)^{1/2} = \frac{1-f}{f}\frac{\theta g_0 \varphi_{A^*}}{[A]_D[Fe(III)](1 + K_q/[Fe(II)])} \quad (11)$$

A2 B2 C1 A1 B2 C2

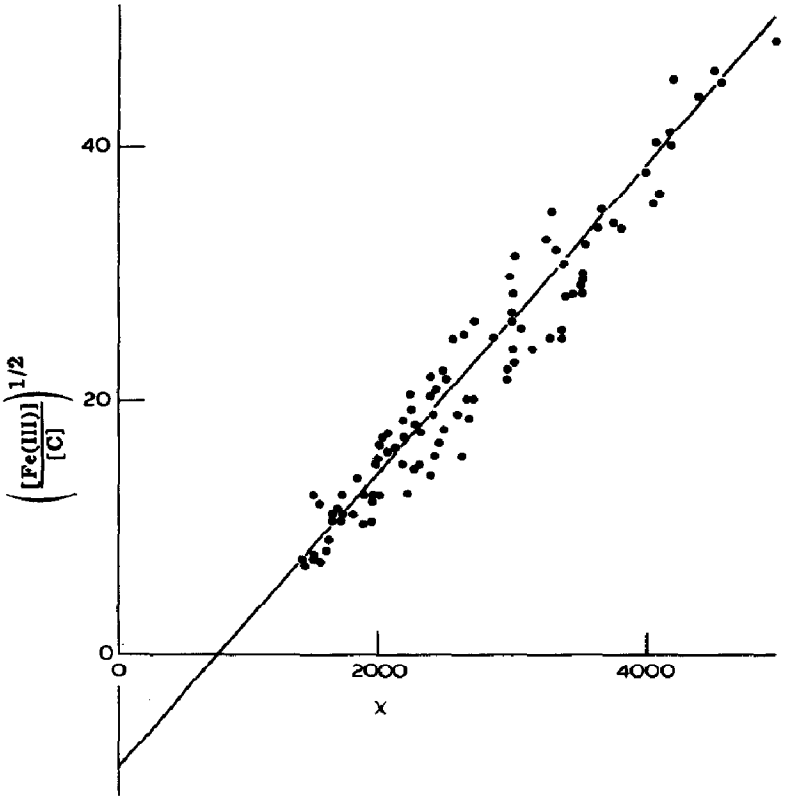

Fig. 3. Plot of all the data in 0.05 M H_2SO_4 according to eqn. (11), where

$$\chi = \frac{1-f}{f}\frac{\theta g_0}{[A]_D[Fe(III)](1 + K_q/[Fe(II)])}$$

This equation is plotted in Fig. 3. All the data for 0.05 M H_2SO_4 lie on a straight line confirming the mechanistic interpretation and the values of K_q. From the intercepts and gradients we find the values of the rate constants given in Table 6. Depending on which term in eqn. (11) is dominant the system will either be A2 B2 C1 or A1 B2 C1. We can therefore read off the value of [Fe(II)]/[C] at which the mechanism changes. These values are given in Table 6. Furthermore from part 5 [1] we have shown that the A1–A2 borderline is given by $\gamma = 2y^2$ or

$$g = 2(k^2_{-1}/k_3)[\mathrm{Fe(III)}]^2 \qquad (12)$$

Values of (k^2_{-1}/k_3) are also given in Table 6. For the system to react by the full disproportionation mechanism A2 B2 C1 we require g to be larger than the critical value given in eqn. (12).

TABLE 6

Values of rate constants and boundary conditions from eqn. (11)

	0.05 M H_2SO_4	0.10 M K_2SO_4
$\varphi_A^{-1} k_{-2}$ (M^{-1} ms^{-1})	0.76	10
$\varphi_A^{-1} k_{-1} (k_{-2}/k_3)^{1/2}$ (M^{-1} s^{-1})	79	1050
[Fe(III)]/[C][a]	90	100
$\varphi_A^{-1} (k^2_{-1}/k_3)$ (M^{-1} s^{-1})[b]	8	110

[a] Critical value of concentration ratio for change of mechanism from A2 B2 C1 to A1 B2 C1.
[b] Value of the constant in eqn. (12) which describes the critical value of g for change in mechanism.

3.5. Implications for photogalvanic cells

In part 5 we showed that for the A1 B2 C1 and A2 B2 C1 mechanisms the optimum production of leucothionine is achieved with the A2 B2 C1 mechanism; this mechanism, assuming $\varphi_B = 1$, has a quantum efficiency φ_c of $\frac{1}{2}$. Hence it is necessary first that φ_B should be close to unity and second that the photochemical flux g should be greater than the critical value given in eqn. (12). For φ_B to be close to unity we require

$$[\mathrm{Fe(II)}] > K_q \approx 1 - 5 \text{ mM}$$

For the second condition we calculate g for AM2 solar radiation $E'(\lambda)$ [7]:

$$g = [\mathrm{A}] \int_{\lambda_1}^{\lambda_2} \frac{\lambda \epsilon_\lambda E_\lambda d\lambda}{Lhc}$$

$$= 3[\mathrm{A}]\ (\mathrm{M}) \qquad (13)$$

Substitution in eqn. (12) together with the values in Table 6 gives us the condition

$$[\mathrm{Fe(III)}\ (\mathrm{mM})] < m_1 \{[\mathrm{A}]\ (\mathrm{mM})\}^{1/2} \qquad (14)$$

where m_1 is 14 in 0.05 M H_2SO_4 and 4 in 0.10 M K_2SO_4. It is also important that the concentration of Fe(III) should not be so large that the lifetime of C is too short for it to reach the electrode; this requires that [7, 8]

$$[\text{Fe(III)}]\,(\text{mM}) < \frac{40}{k_{-2}\ (\text{M}^{-1}\ \text{s}^{-1})} = m_2$$

where m_2 is 50 in 0.05 M H_2SO_4 and 4 in 0.1 M K_2SO_4. In general the larger the concentration of Fe(III) the larger will be the voltage developed by the cell, and there will be less concentration polarization at the dark electrode. Hence it is interesting to enquire which of the conditions in eqns. (14) and (15) is more irksome. The solubility of thionine is only about 1 mM. Hence in 0.1 M K_2SO_4 the two conditions are about equally restrictive while in 0.05 M H_2SO_4 eqn. (14) is more restrictive than eqn. (15). More Fe(III) can be tolerated in 0.05 M H_2SO_4 than in 0.1 M K_2SO_4.

The low solubility of thionine has been recognized [6, 8, 9] as a problem with the iron–thionine system because the radiation cannot be absorbed close enough to the electrode to allow the photogenerated product to react at the electrode. This analysis shows that a more important disadvantage of the low solubility may be that the semithionine intermediates are generated over too wide a region of space to allow them to find each other and form leucothionine. For one electron–two electron photo-redox systems of this type it is important to absorb the radiation in as small a space as possible so that the desired disproportionation reaction can take place efficiently.

In this work we have tested our approach and theory on the iron–thionine system. The same approach and methodology can be used on new systems which have more desirable characteristics and which are therefore better suited for photogalvanic cells.

Acknowledgments

We thank the SRC for research grants and BP for a studentship for WRB. This is a contribution from the Oxford Imperial Energy Group.

References

1 W. J. Albery, M. D. Archer and W. R. Bowen, *J. Photochem.*, *11* (1979) 15 - 25.
2 C. G. Hatchard and C. A. Parker, *Proc. Roy. Soc. London, Ser. A*, 235 (1956) 518.
3 K. Bergmann and C. T. O'Konski, *J. Phys. Chem.*, *67* (1963) 2169.
4 M. I. C. Ferreira and A. Harriman, *J. Chem. Soc. Faraday Trans. 1*, *73* (1977) 1085.
5 C. G. Hatchard and C. A. Parker, *Trans. Faraday Soc.*, *57* (1961) 1093.
6 P. D. Wildes, K. T. Brown, M. Z. Hoffman and N. N. Lichtin, *Solar Energy*, *19* (1977) 79.
7 W. J. Albery and M. D. Archer, *Nature (London)*, *270* (1977) 399.
8 W. J. Albery and M. D. Archer, *J. Electroanal. Chem.*, *86* (1978) 19.
9 D. E. Hall, W. D. K. Clarke, J. A. Eckert, N. N. Lichtin and P. D. Wildes, *Ceramic Bulletin*, *56* (1977) 408.